JOURNAL OF SOLID STATE CHEMISTRY 54, 127–135 (1984)

A Study of the Spinel Materials $LiTi_2O_4$ and $Li_{4/3}Ti_{5/3}O_4$ by Photoelectron Spectroscopy

P. P. EDWARDS,*,† R. G. EGDELL,‡ I. FRAGALA,§
J. B. GOODENOUGH, M. R. HARRISON,* A. F. ORCHARD,
AND E. G. SCOTT

Inorganic Chemistry Laboratory, Oxford University, South Parks Road, Oxford OX1 3QR

Received October 11, 1983; in revised form March 14, 1984

HeI-excited valence-band ultraviolet photoelectron spectra and Mg$K\alpha$-excited Ti-2p X-ray photoelectron spectra are reported for the spinel materials $LiTi_2O_4$ and $Li_{4/3}Ti_{5/3}O_4$. The presence of a Fermi edge in the ultraviolet photoelectron spectrum of $LiTi_2O_4$ confirms the metallic nature of this material, although the measured density of states at the Fermi energy is much lower than that expected from an independent-electron interpretation of the magnetic susceptibility. This difference is attributed to a strong interaction of the conduction electrons with the lattice vibrations. The localization of conduction electrons that occurs in the final state in the Ti-2p X-ray photoelectron spectrum of $LiTi_2O_4$ is attributed to a Coulomb interaction with a core hole.

Introduction

Metallic $LiTi_2O_4$ and insulating $Li_{4/3}Ti_{5/3}O_4$ are the end members of the homogeneity range of the spinel phase in the Li–Ti–O ternary system (*1–3*). The spinel system $Li_{1+x}Ti_{2-x}O_4$ ($0 \leq x \leq 1/3$) has attracted considerable interest because of the high-temperature superconductivity exhibited by compositions with low values of x (*2–4*), and also because of the metal–insulator transition (MIT) exhibited by the system as x increases from 0 to 1/3 (*2–4*). As part of a wider study (*5, 6*) of the electronic properties of this system, we report here the photoelectron spectra of the two end members.

Experimental Methods

Powder samples of $Li_{1+x}Ti_{2-x}O_4$ were prepared by heating together stoichiometric quantities of Li_2TiO_3, Ti_2O_3 (Ventron Alfa, 99%), and TiO_2 (Ventron Alfa, 99.8%) at 800°C either under a dynamic vacuum ($x < 1/3$) or in oxygen ($x = 1/3$) (*5, 6*). The Li_2TiO_3 was itself prepared by heating together stoichiometric quantities of Li_2CO_3 (BDH Analar Grade) and TiO_2 at 800°C in oxygen. The samples were characterized by X-ray powder diffractometry and were subject to investigation by a range of techniques that included diffuse-reflectance

* Present address: University Chemical Laboratory, Cambridge University, Lensfield Road, Cambridge CB2 1EW, UK.

† To whom correspondence should be addressed.

‡ Present address: Department of Chemistry, Imperial College of Science and Technology, London SW7 2AZ, England.

§ Present address: Instituto Dipartimentale di Chimica, Universita di Catania, Viale A. Doria, 8-95125 Catania, Italy.

0022-4596/84 $3.00

spectroscopy, electron spin resonance (ESR) spectroscopy and magnetic-susceptibility measurements (*5, 6*).

Photoelectron (PE) spectra were recorded on a modified AEI ES200B electron spectrometer that has been described elsewhere (*7, 8*). Both 21.2-eV (HeI) and 40.8-eV (HeII) radiation was employed in ultraviolet photoelectron (uv–PE) spectroscopy studies, while unmonochromatized Mg$K\alpha$ radiation (1253.6 eV) was used to excite X-ray photoelectron (X–PE) spectra. The base pressure in the spectrometer was in the high 10^{-10} Torr region.

Immediately after insertion into the spectrometer, $Li_{4/3}Ti_{5/3}O_4$ and $LiTi_2O_4$ gave similar, structureless uv–PE spectra, consistent with an overlayer containing only Ti^{4+} ions. The titanium core levels gave rise to simple spin-orbit doublets in the X–PE spectra. The samples were then cleaned as follows. $Li_{4/3}Ti_{5/3}O_4$ was annealed at 700°C in 10^{-5} Torr of pure oxygen for 1 hr. Annealing under vacuum or hydrogen led to a reduction of the surface of the samples (*5*). $LiTi_2O_4$ was heated slowly to 800°C under vacuum and was annealed at this temperature for periods in excess of 12 hr. Following these procedures, the X–PE spectra were free of signals from elements other than Li, Ti, and O save for a weak C-1*s* peak. The uv–PE spectra of $LiTi_2O_4$ exhibited the structure expected from Ti-3*d* conduction electrons, and the Ti-2*p* core signals in the X–PE spectra contained structure attributable to screening of the Ti-2*p* core hole by conduction electrons (*9*). Heat treatment produces similar improvements in the PE spectra of Ti_2O_3 (*10*). Unfortunately, it proved impossible to obtain reproducible PE spectra from samples with intermediate values of x between 0 and 1/3 (*5*).

After the electron-spectroscopic measurements, X-ray powder diffractometry indicated that no phase changes had been induced by the heat treatment. In particular, the ramsdellite phase formed by heating the spinel phase to temperatures in excess of 900°C (*11, 12*) was absent from the samples.

Results and Discussion

The $Li_{1+x}Ti_{2-x}O_4$ spinel structure. The interpretation of the photoelectron spectra requires the development of a qualitative model for the band structure of the system as shown in Fig. 1. The spinel structure consists of a cubic close-packed array of anions with cations occupying, in an ordered manner, one-eighth of the tetrahedral sites and one-half of the octahedral sites. In the $Li_{1+x}Ti_{2-x}O_4$ system, the covalency of the Ti-3*d* orbitals and the higher charge of the titanium ions gives the titanium ions a strong preference for the octahedral sites relative to the lithium ions. Using X-ray diffraction methods, Johnston (*3*) deduced that the tetrahedral sites in the $Li_{1+x}Ti_{2-x}O_4$ system are indeed occupied entirely by lithium ions and that the octahedral sites are *randomly* occupied by x lithium ions and $(2 - x)$ titanium ions per formula unit.

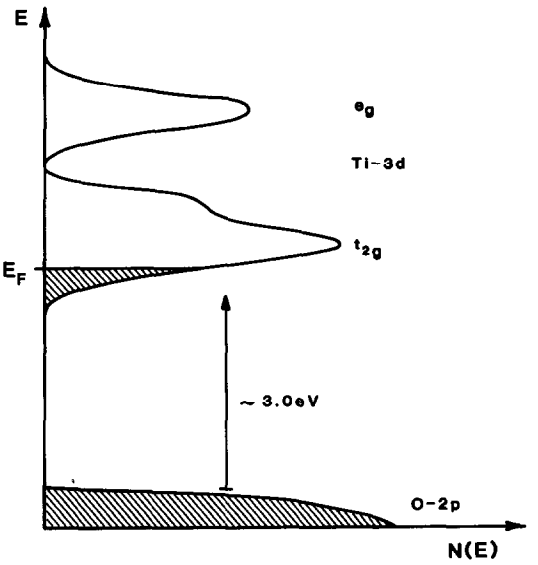

FIG. 1. Schematic band structure for $Li_{1+x}Ti_{2-x}O_4$.

Each titanium ion resides at the center of a trigonally distorted octahedron, and the Ti-3*d* orbitals are split by the cubic component of the crystal field into more stable t_{2g} and less stable e_g orbitals. The t_{2g} orbitals are then further split by the trigonal component of the crystal field, and angular overlap calculations for a Ti^{3+} ion in this structure indicate a trigonal splitting of the order 0.5 eV.[1] The octahedra share edges with each other, and the titanium–titanium separation through the edges of the octahedra decreases from 2.972 Å for $LiTi_2O_4$ to 2.955 Å for $Li_{4/3}Ti_{5/3}O_4$ (*5, 6*). Cation–cation interactions therefore play a dominant role in the formation of the Ti-3*d* conduction band from the t_{2g} orbitals (*13*). The superconducting properties of $LiTi_2O_4$ show that the width of this t_{2g} conduction band is too large to sustain spontaneous magnetism in this material, and a width greater than the trigonal splitting of 0.5 eV may be assumed. Diffuse-reflectance measurements show that the bottom of the t_{2g} conduction band lies approximately 3 eV above the O-2*p* valence band (*5*).

The partial occupation of the octahedral sites by lithium ions changes the number of electrons on the titanium ions. As the fraction of lithium ions on the octahedral sites ($x/(2 - x)$) increases, the average charge of the remaining titanium ions increases from 3.5+ for $LiTi_2O_4$ to 4+ for $Li_{4/3}Ti_{5/3}O_4$. Thus the t_{2g} conduction band is one-twelfth full in $LiTi_2O_4$ and empty in $Li_{4/3}Ti_{5/3}O_4$; the Fermi level, E_F, lies in this band and decreases in energy as x increases. Since $LiTi_2O_4$ is metallic and $Li_{4/3}Ti_{5/3}O_4$ is insulating, a MIT must occur at an intermediate composition if there is a continuous solid solution across the system.

Ultraviolet photoelectron spectra. HeI uv–PE spectra of the materials $LiTi_2O_4$ and $Li_{4/3}Ti_{5/3}O_4$ are shown in Fig. 2. The strong feature peaking at just over 5 eV below the Fermi energy is likely to be associated with the full O-2*p* valence band. The width of this band is difficult to measure from the HeI spectra since strong secondary-electron emission gives rise to a pronounced shoulder on the low-kinetic-energy side of the main peak. However, the intrinsic bandwidth appears to be about 6 eV for both $LiTi_2O_4$ and $Li_{4/3}Ti_{5/3}O_4$. A similar width is found in the HeII spectra where secondary-electron emission is less pronounced. In the case of $Li_{4/3}Ti_{5/3}O_4$, there is only weak emission above the O-2*p* valence

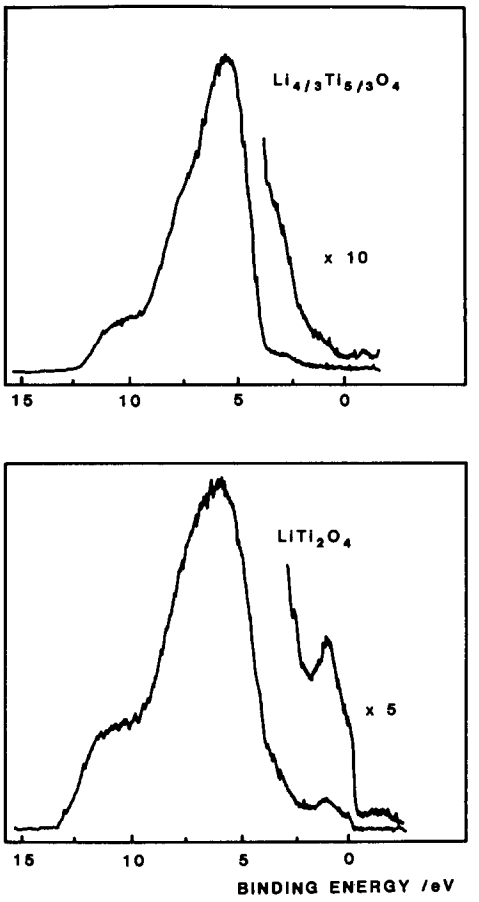

FIG. 2. HeI ultraviolet photoelectron spectra of $Li_{4/3}Ti_{5/3}O_4$ and $LiTi_2O_4$. Binding energies are given relative to the Fermi energy.

[1] Thanks are due to Dr. M. Gerloch, Dept. of Organic and Inorganic Chemistry, Cambridge University, for the use of his computer program "CAMMAG," together with much helpful advice.

band. This weak emission apparently arises from states associated with surface oxygen vacancies, and subsequent annealing of samples under vacuum or hydrogen led to an increase in the intensity of this emission (*5*). Similar structure is found in the spectra of other d^0 oxides (*14, 15*).

The spectrum of $LiTi_2O_4$ differs from that of $Li_{4/3}Ti_{5/3}O_4$ in one significant respect: a prominent peak to low binding energy of the O-2*p* valence band terminates in a sharp edge at the Fermi energy. The width of this edge is estimated to be 125 meV, a value similar to that found for a clean platinum metal sample under identical experimental conditions. This width is determined by the resolving power of the electron-energy analyzer. The additional structure found for $LiTi_2O_4$ is consistent with the partial occupation of a t_{2g} conduction band terminating in a Fermi surface discontinuity in the density of occupied states at the Fermi level. We note that the ratio of the intensities of the emission from conduction and valence bands is 1 : 32, implying that the cross section for ionization of Ti-3*d* conduction electrons is only 0.75 of that for ionization of O-2*p* valence-band electrons. A similar cross section ratio is found by analysis of photoemission data for Ti_2O_3 (*14, 15*).

The shape of the Ti-3*d* region of the spectrum is unusual. The t_{2g} conduction band is only one-twelfth full in $LiTi_2O_4$, and one would expect the highest density of occupied states to occur at the Fermi energy. In the spectrum, however, the peak in the density of occupied states occurs ~1 eV below the Fermi energy. It is possible to explain this unusual shape if the electrons interact with each other or with the lattice vibrations to form quasi-particles with a stabilization energy ~1 eV. The sudden removal of an electron during the photoemission process leaves the system in an excited state, and the system then returns to equilibrium with a relaxation energy ~1 eV. This relaxation shifts the photoemission peak to higher binding energy, and consequently lowers the measured density of states at the Fermi energy (*16*). An interaction of the electrons with each other or with the lattice vibrations should also result in an enhancement of the magnetic susceptibility and conduction-electron heat capacity over the respective independent-electron values. This is discussed below.

Toward the bottom of the t_{2g} conduction band in $LiTi_2O_4$, the Bloch states are predominantly of Ti-3*d* character; the hybridization with O-2*p* states increases slowly toward the top of the conduction band. In view of this, and the closely similar values of ionization cross sections for Ti-3*d* conduction electrons and O-2*p* valence-band electrons, one expects variations in the photoionization matrix elements across the occupied part of the conduction band to be rather small. If we make the additional assumption that there is no modulation with photoelectron energy in the density of final states, we can normalize the area of the conduction band in our spectra to the electron concentration implied by the chemical composition $LiTi_2O_4$. It is then possible to estimate the *photoemission* density of states at the Fermi energy, $N_{pe}(E_F)$, from the measured height of the Fermi surface discontinuity in the spectra. With this procedure we arrive at the value of $N_{pe}(E_F)$ given in Table I.

Our estimate is nearly a factor of three lower than the *free-electron* density of states at the Fermi energy, $N_0(E_F)$, in a parabolic band containing electrons with the free-electron mass, m_0 (Table I). It is also approximately a factor of 30 lower than the *independent-electron* density of states at the Fermi energy, $N_x(E_F)$, deduced by Johnston (*3*) from an analysis of magnetic susceptibility data for $LiTi_2O_4$ (Table I). Johnston's calculations are outlined in the Appendix; it is assumed that the high value of the magnetic susceptibility arises from the effects of a narrow t_{2g} conduction band.

TABLE I

DENSITY OF STATES AT THE FERMI ENERGY IN $LiTi_2O_4$

Technique	$N(E_F)$ states (eV-formula unit)
Photoemission measurements (present work)	0.25
Free-electron theory	0.72
Magnetic susceptibility measurements (*3*) using Eq. (4)	6.8
Heat capacity measurements (*4*) using Eq. (6)	9.1

Both the electron effective mass, m^*, and the density of states would then be increased.

This discrepancy in the values of the density of states at the Fermi energy deduced by the different techniques contrasts with the situation in Na_xWO_3, where there is excellent agreement between the values of $N_{pe}(E_F)$ estimated from photoemission experiments and the values of $N_x(E_F)$ deduced from a similar analysis of magnetic susceptibility data (*17, 18*). It suggests that the photoemission density of states at the Fermi energy in $LiTi_2O_4$ may indeed be reduced by the quasi-particle mechanism outlined above, and that the magnetic susceptibility of $LiTi_2O_4$ is enhanced, not by virtue of a high effective mass arising from a narrow t_{2g} conduction band but instead by electron interactions with other electrons or with lattice vibrations. The *actual* density of states at the Fermi energy may well be comparable to the free-electron value.

Interactions with other electrons are expected to be comparatively small since there is a nonintegral number (0.5) of conduction electrons per titanium ion in $LiTi_2O_4$ (*19*). Instead, the electrons are more likely to interact with the lattice vibrations to form small polarons (*19*). Such interactions are consistent with the high superconducting transition temperature observed in this material, and also with the formation of electron pairs in other titanium oxides such as Ti_4O_7 (*20, 21*). In fact, Ti_4O_7 has the same number of conduction electrons per titanium ion as $LiTi_2O_4$, but at low temperatures these electrons are localized as diamagnetic Ti^{3+}–Ti^{3+} dimers. It is well established that a strong interaction of the electrons with the lattice vibrations is necessary for the stability of these electron pairs (*22*).

Other transition-metal oxides exhibit similar evidence of electron interactions. In the metallic phase of V_2O_3, for example, a comparison between the photoemission density of states at the Fermi energy (*8*) and the density of states deduced from magnetic susceptibility data (*23*) implies an enhancement of the magnetic susceptibility density of states by a factor of approximately 140 if an independent-electron model is used. However, measurements of the low-frequency optical reflectivity spectrum of V_2O_3 suggest that $m^* \sim 9m_0$ (*19*). Thus only a small part of the enhancement in this material may be ascribed to a narrow conduction band. Mott (*19*) has argued in favor of a Brinkman–Rice enhancement mechanism (*24, 25*) with possibly some additional enhancement due to small polaron formation. Brinkman–Rice enhancement is found in materials with a half-filled conduction band where the electron interactions are associated with an incipient antiferromagnetism. Both the magnetic susceptibility and the conduction-electron heat capacity are predicted to be strongly enhanced.

In the metallic phase of VO_2, a similar comparison between the photoemission density of states at the Fermi energy (*8*) and the density of states deduced from magnetic susceptibility data (*23*) implies an enhancement of the magnetic susceptibility density of states by a smaller factor of approximately 70 if an independent-electron model is used. Measurements of the low-frequency optical reflectivity spectrum of

VO_2 suggest that $m^* \sim 3m_0$ and Mott (*19*) has concluded that the electron interactions are strong in VO_2 although weaker than the interactions in V_2O_3.

Ti-2p X-ray photoelectron spectra. Photoelectron spectra of the Ti-2*p* core levels in $LiTi_2O_4$ and $Li_{4/3}Ti_{5/3}O_4$ are shown in Fig. 3. As expected the spectrum of the d^0 material $Li_{4/3}Ti_{5/3}O_4$ is a simple spin-orbit doublet, the $^2P_{3/2}:{}^2P_{1/2}$ intensity ratio being close to the expected value of 2:1. In contrast the spectrum of $LiTi_2O_4$ apparently consists of two overlapping spin-orbit doublets, with the positions of the peaks inferred from a heuristic curve analysis being given in the figure. Data of this sort have been taken to indicate the presence of two distinct oxidation states for the transition-metal atom in the *initial* state of the system (*26*). However, the superconducting nature of $LiTi_2O_4$ clearly demonstrates the itinerant nature of the conduction electrons, and we prefer an alternative interpretation of our data along the following lines (*9, 27–29*).

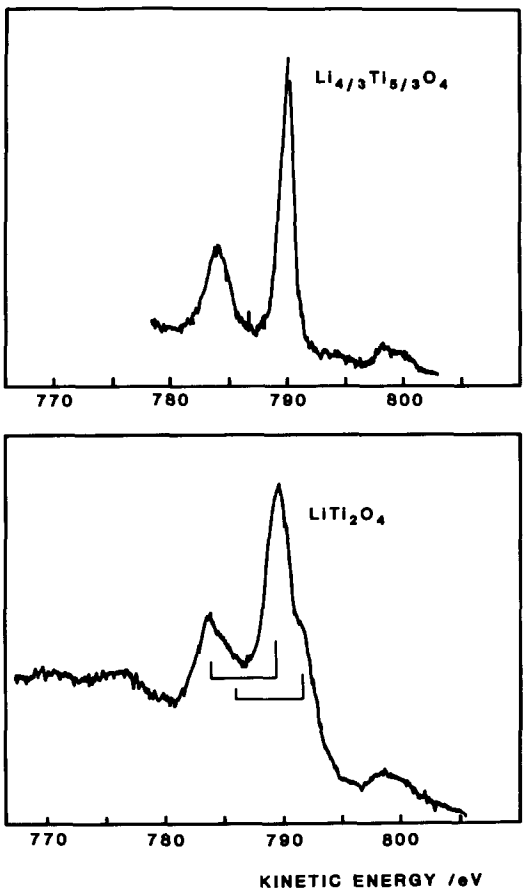

FIG. 3. Ti-2*p* region in the Mg*Kα* X-ray photoelectron spectra of $Li_{4/3}Ti_{5/3}O_4$ and $LiTi_2O_4$. Peak positions inferred from a heuristic analysis of the data for $LiTi_2O_4$ are indicated in the figure.

Ionization of a titanium core subshell in a narrow-band metallic material such as $LiTi_2O_4$ produces a strong electrostatic perturbation that disengages one of the ionized-atom orbitals from the conduction band. This localized Ti-3*d* state will lie well below the Fermi level, and the titanium site in question will behave as an electron trap. Two different *final* states are then accessible, corresponding to the trap being: (1) occupied and (2) empty. Since the localized Ti-3*d* wavefunctions are necessarily orthogonal to the Bloch wavefunctions of the conduction band, cases (1) and (2) involve the creation of $*Ti^{4+}$ (d^1) and $*Ti^{5+}$ (d^0) species, respectively, where the asterisk indicates the presence of a core-hole.

According to a model developed by Kotani and Toyazawa (*30*), the "screened" final state for an occupied trap gives rise to an asymmetric band to lower binding energy of the lifetime-broadened peak associated with the "unscreened" final state. In this model, the relative probabilities of reaching the "screened" and "unscreened" final states depend on projections of the differing final-state wavefunctions onto a Koopman's state wavefunction. Calculations indicate that the final-state intensity ratio is a sensitive function of the bandwidth in the initial state relative to the magnitude of the hole-electron Coulomb integral that effects final-state localization (*31, 32*). In the mixed-valence initial-state interpretation, the intensity ratio between d^1 and d^0 final-state peaks should reflect the formal $Ti^{3+}:Ti^{4+}$

initial-state ratio, which for the case of $LiTi_2O_4$ is 1:1. Our observation that the "screened":"unscreened" intensity ratio is approximately 1:2 lends strong support to the final-state localization model and suggests a hole-electron Coulomb integral significantly larger than the bandwidth (*31, 32*).

Concluding Remarks

Photoelectron spectra of the two end members of the spinel phase $Li_{1+x}Ti_{2-x}O_4$ are compatible with a qualitative band structure similar to those developed for other transition-metal oxides (*13*). In particular the observation of a discontinuity at the Fermi energy in the occupied density of states for $LiTi_2O_4$ is consistent with the metallic nature of this material. However, the measured density of states at the Fermi energy is much lower than that expected from an independent-electron interpretation of the magnetic susceptibility of this material. We believe that this difference may be attributed to a strong interaction of the conduction electrons with the lattice vibrations. Complex core-level structure in the Ti-2*p* X-ray photoelectron spectrum of $LiTi_2O_4$ suggests the presence of localized d^1 and d^0 states. However, we believe that the conduction-electron localization does not precede core ionization, but rather is a consequence of it.

Appendix

Johnston's estimate of $N_x(E_F)$ from magnetic susceptibility data was based on the following independent-electron analysis. Temperature-dependent molar susceptibilities, χ, in the spinal system were separated into a Curie–Weiss term, $C_m/(T + \theta)$, and a weakly temperature-dependent term, $f(T)$:

$$\chi = C_m/(T + \theta) + f(T). \quad (1)$$

The Curie–Weiss contribution to the magnetic susceptibility arises from localized Ti^{3+} moments in the sample present at a molar concentration of approximately 1% (*5, 6*). The term $f(T)$ was assumed to be an essentially temperature-independent, conduction-electron magnetic susceptibility, χ_{ce}, that included both Pauli paramagnetic and Landau diamagnetic terms:

$$\chi_{ce} = \beta^2(m^*/m_0)N_0(E_F)(1 - m_0^2/3m^{*2}), \quad (2)$$

where β is the Bohr magneton, m^* the conduction-electron effective mass, m_0 the free-electron mass, and $N_0(E_F)$ the *free-electron* density of states at the Fermi energy in a parabolic energy band:

$$N_0(E_F) = \frac{4m_0(3\pi^2 n)^{1/3}}{h^2}, \quad (3)$$

where n is the concentration of conduction electrons, and h is Planck's constant. Equations (2) and (3) determine the mass enhancement, m^*/m_0, arising from a narrow t_{2g} conduction band. The *independent-electron* density of states at the Fermi energy deduced from magnetic susceptibility measurements is then given by the relation

$$N_x(E_F) = (m^*/m_0)N_0(E_F). \quad (4)$$

Our magnetic susceptibility data for $LiTi_2O_4$ (*5, 6*) is similar to that found by Johnston (*3*). We note here that, in agreement with Fig. 7 of his paper (*3*), the contribution $f(T)$ to the magnetic susceptibility shows a noticeable temperature dependence that may be suitably parameterized in the form

$$f(T) = A_m + B_m T, \quad (5)$$

where $A_m = 2.13 \times 10^{-3}$ J T^{-2} $mole^{-1}$ and $B_m = -8.8 \times 10^{-7}$ J T^{-2} $mole^{-1}K^{-1}$. Using this value of A_m, it is possible to calculate a mass enhancement $m^*/m_0 = 9.4$ and the corresponding independent-electron density of states at the Fermi energy given in Table I.

This calculation, however, supposes a

mass enhancement arising solely from a narrow t_{2g} conduction band; it does not allow for an additional enhancement of the magnetic susceptibility due to electron interactions. If we assume that the *actual* density of states at the Fermi energy is comparable to the free-electron value (so that $m^* \sim m_0$), and if the free-electron density of states is used in Eq. (2) to calculate the free-electron magnetic susceptibility, an enhancement factor ~10 due to electron interactions is required to explain the experimental data. As indicated in the discussion, these electron interactions are anticipated to be with the lattice vibrations.

Similar arguments apply to the conduction-electron heat capacity (γ_{ce}) above the superconducting transition measured by Johnston *et al.* (*4*). An estimate of the independent-electron density of states at the Fermi energy, $N_\gamma(E_F)$, deduced from heat capacity measurements may be obtained through the relation

$$\gamma_{ce} = \pi^2 k_B^2 N_\gamma(E_F)/3, \qquad (6)$$

where k_B is Boltzmann's constant. The value deduced from the heat capacity data is approximately one-third larger than the value deduced from the magnetic susceptibility data (Table I). However, this calculation depends upon the same assumption of independent electrons as outlined above. If the free-electron density of states is used in Eq. (6) to calculate the free-electron heat capacity, an enhancement factor ~10 due to electron interactions is again required to explain the experimental data. It thus appears that both χ_{ce} and γ_{ce} would need to be enhanced by a similar factor ~10.

Acknowledgments

We thank the SERC for financial support, and Mr. Dave Spilsbury for assistance in the early stages of this work. We also thank the referees for their constructive comments on this manuscript.

References

1. A. Deschanvres, B. Raveau, and Z. Sekkal, *Mater. Res. Bull.* **6,** 699 (1971).
2. D. C. Johnston, H. Prakash, W. H. Zachariasen, and R. Viswanathan, *Mater. Res. Bull.* **8,** 777 (1973).
3. D. C. Johnston, *J. Low-Temp. Phys.* **25,** 145 (1976).
4. R. W. McCallum, D. C. Johnston, C. A. Luengo, and M. B. Maple, *J. Low-Temp. Phys.* **25,** 177 (1976).
5. M. R. Harrison, D. Phil. thesis, Oxford University (1981).
6. M. R. Harrison, P. P. Edwards, and J. B. Goodenough, *J. Solid State Chem.* **54,** 134 (1984).
7. N. Beatham and A. F. Orchard, *J. Electron Spectrosc. Relat. Phenom.* **16,** 77 (1979).
8. N. Beatham, I. L. Fragala, A. F. Orchard, and G. Thornton, *J. Chem. Soc. Faraday Trans. II* **76,** 929 (1980).
9. N. Beatham, P. A. Cox, R. G. Egdell, and A. F. Orchard, *Chem. Phys. Lett.* **69,** 479 (1980).
10. N. Beatham, A. F. Orchard, and G. Thornton, *J. Phys. Chem. Solids,* in press.
11. U. Roy, K. Petrov, I. Tsolovski, and P. Peshev, *Phys. Status Solidi A* **44,** K25 (1977).
12. K. Petrov and I. Tsolovski, *Phys. Status Solidi A* **58,** K85 (1980).
13. J. B. Goodenough, *Prog. Solid State Chem.* **5,** 145 (1971).
14. V. E. Henrich, G. Dresselhaus and H. J. Zeiger, *Phys. Rev. B* **17,** 4908 (1978).
15. V. E. Henrich, G. Dresselhaus, and H. J. Zeiger, *Phys. Rev. Lett.* **36,** 1335 (1976).
16. G. A. Sawatzky and E. Antonides, *J. Physique C* **4,** 117 (1976).
17. R. G. Egdell and M. D. Hill, *Chem. Phys. Lett.* **88,** 503 (1982).
18. R. G. Egdell and M. D. Hill, *Chem. Phys. Lett.* **85,** 140 (1982).
19. N. F. Mott, "Metal–Insulator Transitions," Taylor & Francis, London (1974).
20. C. Schlenker and M. Marezio, *Philos. Mag. Part B* **42,** 453 (1980).
21. C. Schlenker, S. Ahmed, R. Buder, and M. Gourmala, *J. Phys. C* **12,** 3503 (1979).
22. B. K. Chakraverty, M. J. Sienko, and J. Bonnerot, *Phys. Rev. B* **17,** 3781 (1978).
23. C. N. R. Rao and G. V. Subba Rao, "Transition Metal Oxides," NSRD-NBS 49, U.S. Govt. Printing Office, Washington, D.C. (1974).
24. W. F. Brinkman and T. M. Rice, *Phys. Rev. B* **2,** 1324 (1970).
25. W. F. Brinkman and T. M. Rice, *Phys. Rev. B* **2,** 4302 (1970).

26. B. A. DE ANGELIS AND M. SCHIAVELLO, *Chem. Phys. Lett.* **58,** 249 (1976).
27. J. N. CHALZALVIEL, M. CAMPAGNA, G. K. WERTHEIM AND H. R. SHANKS, *Phys. Rev. B* **16,** 697 (1977).
28. J. C. FUGGLE, F. U. HILLEBRECHT, Z. ZOLNIEREK, R. LASSER, CH. FREIBURG, O. GUNNARSSON AND K. SCHONHAMMER, *Phys. Rev. B* **27,** 7330 (1983).
29. G. K. WERTHEIM, *Chem. Phys. Lett.* **65,** 377 (1979).
30. A. KOTANI AND Y. TOYAZAWA, *J. Phys. Soc. Jpn.* **37,** 912 (1974).
31. P. A. COX, *in* "Proceedings, X-80 Conference on X-Ray and Inner-Shell Physics of Atoms and Solids, Plenum, New York (1981).
32. G. A. SAWATZKY AND A. LENSELINK, *J. Chem. Phys.* **72,** 3748 (1980).